

Mottness induced phase decoherence suggests Bose-Einstein condensation in overdoped cuprate high-temperature superconductors

Zi-Jian Lang (郎子健),¹ Fan Yang (杨帆),² and Wei Ku (顧威)^{1,3,*}

¹*Tsung-Dao Lee Institute & School of Physics and Astronomy,
Shanghai Jiao Tong University, Shanghai 200240, China*

²*School of Physics, Beijing Institute of Technology, Beijing 100081, China*

³*Key Laboratory of Artificial Structures and Quantum Control (Ministry of Education), Shanghai 200240, China*

(Dated: July 19, 2022)

Recent observations of diminishing superfluid phase stiffness in overdoped cuprate high-temperature superconductors challenges the conventional picture of superconductivity. Here, through analytic estimation and verified via variational Monte Carlo calculation of an emergent Bose liquid, we point out that Mottness of the underlying doped holes dictates a strong phase fluctuation of the superfluid at moderate carrier density. This effect turns the expected doping-increased phase stiffness into a dome shape, in good agreement with the recent observation. Specifically, the effective mass divergence due to “jamming” of the low-energy bosons reproduces the observed nonlinear relation between phase stiffness and transition temperature. Our results suggest a new paradigm, in which the high-temperature superconductivity in the cuprates is dominated by physics of Bose-Einstein condensation, as opposed to pairing-strength limited Cooper pairing.

PACS numbers: 74.72.-h, 74.20.Mn, 74.40.Kb, 74.20.Rp

Discovered almost thirty years ago[1], the exotic phenomenon of high-temperature superconductivity (HT-SC) in the cuprates still remains puzzling to researchers. Conventional superconductivity, a state of the matter that shows no resistance in conducting current, is well described by the standard “BCS” theory[2] via weakly bound “Cooper pairs” that fluctuate in amplitude. On the other hand, the HT-SC in cuprates shows qualitatively different behavior. For example, in the weakly hole doped (“underdoped”) region, the isotope effect increases dramatically and yet the corresponding superconducting transition temperature T_c decreases [3] instead. The observed superconducting gap Δ_0 in the cuprates is typically significantly larger than the canonical value of twice the transition temperature $\sim 2k_B T_c$ in BCS theory [4, 5]. During the phase transition, the measured specific heat shows two clear kinks 10K apart [6], qualitatively different from a standard second-order phase transition from the BCS theory. Furthermore, in the underdoped region, the low-temperature specific heat shows no T^2 contribution expected from the observed d -wave quasiparticles, but only a dominant T^3 instead [6]. In addition, the observed upper critical field H_{c2} does not saturate at low temperature and sometimes even exceeds the Pauli limit [7]. These qualitative distinct features indicates clearly that the HT-SC in the cuprates is of a different nature.

A significant step forward came with the realization of a different physical regime where the fluctuation is predominately in the superconducting phase[8, 9] rather than its amplitude. In that case the superconducting transition temperature T_c would be determined by the phase stiffness, as opposed to the strength of the pairing. This regime is arguably unavoidable in the low doping

δ (low carrier density n) regime of cuprates, given the canonical conjugation between carrier density and phase ϕ , $\Delta n \Delta \phi \sim \hbar$ [9]. This crucial realization seems to provide a very natural explanation of the generic “dome” shape of superconducting transition temperature in the cuprates: As shown schematically in Fig. 1(a), in the underdoped side, T_c increases as the phase stiffness grows at higher carrier density (grey dotted line), while in the overdoped side T_c decreases due to reducing pairing interaction (grey dashed line) as in the BCS theory.

However, recent measurement [10] of penetration depth λ challenges this traditional picture. Surprisingly, the low-temperature superfluid phase stiffness ($\propto \lambda^{-2}$) also forms a dome shape against doping, qualitatively different from the simple proportionality to carrier density [11] expected in the pairing strength-limited BCS theory. Furthermore, the low-temperature phase stiffness even scales with T_c in the overdoped regime, obeying the same universal Uemura-relation [12–14] well-known in the underdoped regime. Since this relation implies a phase coherence-limited superconductivity, this new data apparently reveals that even in the overdoped side, the dominant physics is still the phase fluctuation!

In fact, several previous studies already raised similar doubts against the common lore that at least in the overdoped regime the superconductivity can still be described by pairing strength-limited BCS-like theories. As shown in Fig. 1(b), angular resolved photo-emission spectroscopy (ARPES) observed[15, 16] a nearly doping independent superconducting gap Δ near momentum $(\pi/2, \pi/2)$ for almost the entire doping range, in great contrast to the expected proportionality to T_c in the BCS theory. Similarly, Fig. 1(d) shows that even earlier, the observed momentum-dependence of superconducting

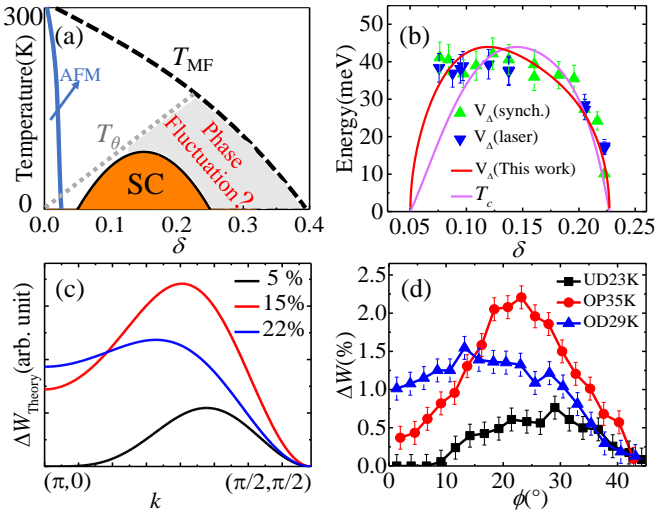


FIG. 1: Indications of the essential role of phase fluctuation even in the overdoped cuprates. (a) Schematic phase diagram of hole-doped HTSC. Beyond the antiferromagnetic (AFM) phase at very low doping, the superconductivity exists in a “dome” region of the phase diagram, much smaller than the one predicted by the VMC calculation. This suggests that below the classical phase coherent temperature, T_θ , additional phase fluctuation must exist in the region in grey. (b) Observed superconducting gap size (triangles) near momentum $(\pi/2, \pi/2)$ [15, 16] displays a doping dependence very different from that of superconducting temperature (purple line), but well captured by $\Delta \propto (1 - 2\delta)\sqrt{T_c}$ (red line). Normalized spectral weight transfer ΔW from condensed EBL (c) and ARPES [17] (d) both show a d -wave form distinct from the $\cos(k_x) - \cos(k_y)$ form of the superconducting order parameter expected in BCS-like theories.

gap-induced weight transfer deviates qualitatively from the well-established $d_{x^2-y^2}$ form of the superconducting order parameter, also from the underdoped regime *all the way to the overdoped regime*. Both observations suggests more commonality between the underdoped regime and the overdoped one than previously expected. Consistently, variational Monte-Carlo (VMC) calculations [18–20], which ignore quantum phase fluctuation, all found that the pairing still exists beyond 25% doping [black dashed line in Fig. 1(a)]. In this case, the entire superconducting dome would be deep inside the pairing region of the phase diagram, and thus the demise of superconductivity must be controlled by additional phase fluctuation.

But, how is it even possible to host such a strong phase fluctuation at such high carrier density? Particularly in the overdoped regime, how can the phase quantum-fluctuates even stronger with increased carrier density, as to wipe out superconductivity at roughly $\delta > 25\%$? Why is this critical doping level seemingly universal across different families of cuprates? What determines this special doping level? What is the origin of the striking similarity between the underdoped and overdoped regime, especially near the quantum critical points (the

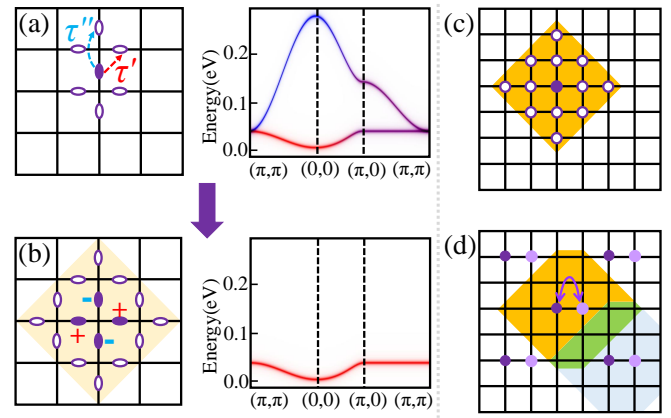


FIG. 2: Model of an emergent Bose liquid. (a) Hopping of a bond-centered boson (solid ellipse) to nearest τ' and next nearest τ'' neighboring bonds (empty ellipse), giving rise to a two-band dispersion (right panel), colored in red/blue to reflect the d - and s -wave nature. (b) d -wave boson corresponding to the low-energy effective one-orbital description with one band dispersion (right panel), requiring 16 forbidden bonds. (c) Extended hard-core constraint among site-centered d -wave bosons, up to third neighboring sites. (d) Simple estimation of highest boson density with minimal non-zero kinetic energy allowing hopping within two-sites on average.

end of the dome) $\delta \sim 5\%$ and 25% ? Finally and most importantly, what essential nature do these puzzles reveal about the unconventional high-temperature superconductivity in the cuprates?

Here we show that all these important questions can be answered naturally in the scenario of the emergent Bose liquid (EBL) [21–23]. In this low-energy effective theory the doped holes are assumed to be tightly bound into local nearest neighboring pairs due to various higher-energy physics, for example, exclusion of double occupation [24, 25], two-dimensional short-range antiferromagnetic correlation [26] and bi-polaronic correlation [27]. The resulting pivoting motion of the emergent bosons is then described by a bond-centered checkerboard lattice (a two-orbital Hamiltonian corresponding to the vertical and horizontal bonds) as shown in Fig. 2(a):

$$H = \sum_{\langle l, l' \rangle} \tau_{ll'} b_l^\dagger b_{l'}^\dagger \quad (+ \text{ constraint}) \quad (1)$$

where b_l denotes the annihilation of a boson located at bond l , and $\tau_{ll'} = \tau'$ or τ'' is the fully dressed kinetic process involving nearest and second nearest neighboring bonds (which was previously extracted from ARPES dispersion data [21].) It is important to note that the emergent bosons have an “extended hard-core” constraint: all nearest and second nearest neighboring bonds [c.f.: empty ellipses in Fig. 2(a)] are excluded from other bosons, due to the double-occupancy constraint of the underlying doped holes in a Mott insulator. This effective short-range repulsion helps provide the phase stiff-

ness of superfluidity and prevents phase separation due to clustering of the emergent bosons.

Previously this model was shown to offer a simple explanation for the disappearance of superfluidity in cuprates at $\delta \sim 5\%$, as the effective mass of the emergent boson diverges [22]. (The same study also suggested a scenario for the lack of superfluidity below 5% doping.) In a related study, a second kind of “superconducting gap” was found in the quasi-particle spectrum, resulting from coherent *kinetic* scattering against the Bose-Einstein condensation (BEC) of the EBL [21]:

$$\Delta_{\mathbf{k}}(T) \sim f_d(k) \cdot (\epsilon_k - \epsilon_0) \sqrt{n_0(T)} \quad (2)$$

where $f_d(k) = \frac{1}{2}[\cos(k_x) - \cos(k_y)]$ gives the momentum dependent *d*-wave form factor of the order parameter and $n_0(T)$ the temperature-dependent condensation density. $\epsilon_k - \epsilon_0$ denotes the quasi-particle energy measured from the low-energy band center, and signifies the kinetic origin of the gap (as opposed to the pairing potential). Beyond the “Fermi arc”, where ϵ_k moves from the chemical potential toward the band center, it provided additional momentum dependence [21] that reproduced nicely the ARPES measurements [17] at various doping levels [c.f. Fig. 1(c).]

We first observe that this model actual “predicted” naturally the above-mentioned nearly doping independent superconducting gap in ARPES measurements [15, 16]. Since the quasi-particles on the Fermi arc are at the chemical potential μ , $\epsilon_k - \epsilon_0$ is given by $\mu - \epsilon_0 \propto 1 - 2\delta$ upon hole doping into the quasi-2D singlet band of the cuprates. Away from the ends of the dome, in the absence of strong quantum fluctuation, the condensation density $n_0(T=0)$ is roughly proportional to the superfluid density, $n_s(T=0) \propto T_c$. Together, this gives a weakly doping dependent near-node gap scale $V_{\Delta} \propto (1 - 2\delta)\sqrt{T_c}$, very similar to the experiments shown in Fig. 1(b), but in great contrast to the stronger dome shape of T_c . Particularly, notice that the $1 - 2\delta$ factor shifts the maximum of V_{Δ} to a significantly lower doping $\delta \sim 0.12$, compared to T_c . Similar to the above mentioned deviation from *d*-wave form of the gap, this again reflects the kinetic nature of the scattering gap absent in typical pairing scenario.

Concerning the main puzzles of the strong phase fluctuation and diminishing superfluidity density at overdoped regime, we will now show that the EBL also provides a simple resolution through its “extended hard-core constraint”. Focusing on the lower-energy *d*-wave bosons relevant to the BEC in Fig. 2(a), we first integrate out the higher-energy *s*-wave bosonic degrees of freedom. The resulting one-orbital Hamiltonian

$$\tilde{H} = \sum_{\langle i, i' \rangle} \tilde{\tau}_{ii'} d_i^{\dagger} d_{i'} \quad (+ \text{ interaction \& constraint}) \quad (3)$$

corresponds to larger local *d*-wave Wannier functions [cf: Fig. 2(b)] that can hop to the first, second and third

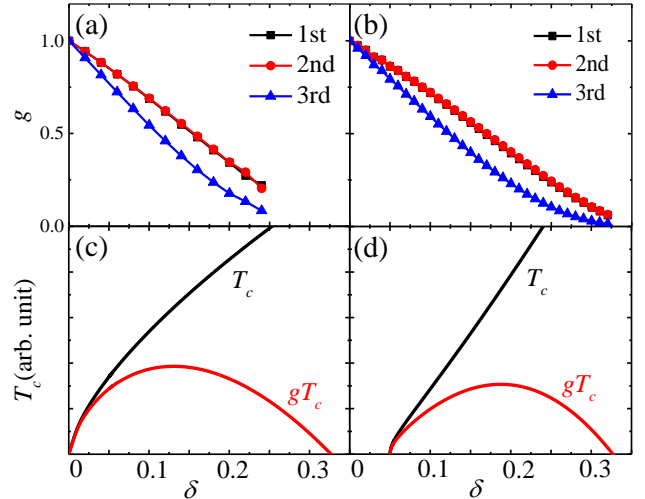


FIG. 3: Gutzwiller *g*-factor of the hopping parameters, calculated from (a) statistical counting and (b) VMC. (c) Theoretical (black line) and renormalized (red line) transition temperature T_c estimated from standard free Bose gas and the Gutzwiller approximation. (d) same as (c) but with realistic mass from Ref. [21, 22] containing additional mass divergence around $\delta \sim 5\%$ doping.

neighbors with $\tilde{\tau}_{ii'}$ with a correspondingly more extended hard-core constraint over 16 bonds. Here d_i^{\dagger} denotes creation of a *d*-wave boson at site i . As highlighted in Fig. 2(c), this constraint forbids occupation of 12 surrounding sites by other low-energy *d*-wave bosons.

Such a large extended hard-core implies that the essential kinetic processes will be easily renormalized at moderate density due to blocking and jamming between the low-energy *d*-wave bosons. Figure 2(d) shows a simple estimation of the special case, in which each of the bosons reach minimum non-zero mobility on average, being able to hop back and forth between two sites. The corresponding density, 2 holes (1 boson) / 8 atomic sites = 25%, marks the approximate maximum doping level of superfluidity, above which the *d*-wave bosons become nearly impossible to move and thus unable to maintain phase coherence. Interestingly, this 25% coincides very well with the experimentally observed end of the superconducting dome in overdoped cuprates in general [28]. Therefore, this mechanism offers a simple and natural explanation of the key puzzle of strong phase fluctuation in the overdoped cuprates.

We employ the well-known Gutzwiller *g*-factor approximation [29, 30] $\tilde{\tau}_{ii'} \rightarrow g_{ii'} \tilde{\tau}_{ii'}$ as the simplest way to capture this renormalization of the kinetic process. The *g*-factors are calculated via two numerical approaches [31]. First, we count statistically the probability of each hopping under the constraint at various doping level. Figure 3(a) shows that the resulting *g*-factors are approximately $g \sim 1 - \delta/0.3$. Second, we calculate the *g*-factor using VMC based on a noninteracting BEC wavefunction under the constraint. The resulting *g*-factors in Fig 3(b) resemble Fig 3(a) very well. As expected, both results

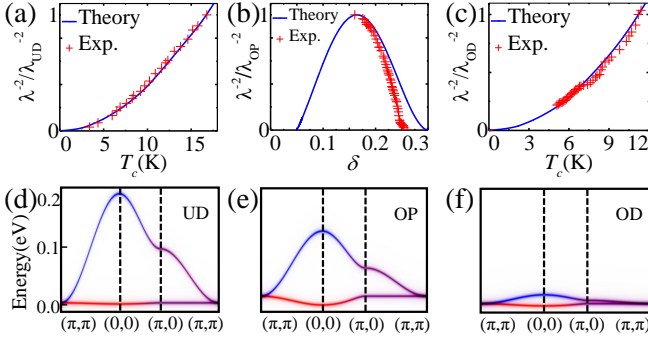


FIG. 4: (a) Correlation between low-temperature superfluid stiffness λ^{-2} and superconducting transition temperature T_c near 5% quantum phase transition point [22, 32], normalized by λ_{UD}^{-2} at $T_c = 17$ K. (b) Superfluid phase stiffness λ^{-2} vs doping level δ showing a dome shape [10], normalized by λ_{OP}^{-2} at $\delta = 0.16$. Theoretical overestimation in the overdoped region is expected from the Gutzwiller treatment. (c) same as (a) for the overdoped region [10], normalized by λ_{OD}^{-2} at $T_c = 11$ K. (d)-(f) Renormalized band structure of EBL near $\sim 5\%$, $\sim 15\%$, and $\sim 25\%$ doping, showing similar effective mass divergence of low-energy band near transition points, but with distinct higher energy features.

decrease rapidly and become rather small beyond 25%.

We now demonstrate the “dome” shape of T_c with our simple picture. Estimated from the standard BEC of a uniform boson gas, the condensation temperature $T_c \propto n^{2/3}/m^*$ is a simple function of density n and effective mass m^* . Obviously, following $\tilde{\tau}$, $1/m^*$ and T_c are also renormalized by g . Figure 3(c) plots $T_c \propto \delta^{2/3}$ (in black) and the renormalized $T_c \rightarrow gT_c$ (in red). Indeed gT_c is strongly suppressed at higher doping and eventually vanishes around 30%, where m^* diverges in an average sense. (The Gutzwiller approximation is expected to underestimate the short-range fluctuation when the jamming becomes severe at high density, resulting in a slight overestimation of the persistence of the superfluidity beyond 25% doping.) If we further incorporate the previously proposed doping dependent mass of the boson [22], which contains an additional mass divergence at around 5% due to level crossing, the gT_c in Fig. 3(d) reproduces the experimentally observed dome shape quite well. In short, the phase fluctuation can indeed grow in the overdoped regime when the suppression of kinetic processes overcomes the increasing density.

Similarly, the low-temperature limit of the phase stiffness λ^{-2} would also suffer from the jamming reduced kinetic process. Phase stiffness $\lambda^{-2} \propto n_s/m^*$ is proportional to the superfluid density n_s . Near the above mentioned mass divergence dictated quantum phase transition points, $n_s \propto (1/m^*)^\beta \delta$ must vanish with $1/m^*$ with a exponent $\beta > 0$, leading to $\lambda^{-2} \propto (1/m^*)^{1+\beta} \delta$. Figure 4(b) shows that this phase stiffness indeed forms a dome shape, vanishing at around $\delta \sim 5\%$ and $\sim 30\%$.

Particularly, due to the extended hard-core constraint of the EBL, the phase stiffness reduces in the overdoped regime against the growing density, as observed in recent experiments [10, 11]. (Our results’ deviation from experiment merely reflects the above-mentioned overestimation of phase coherence at high doping in our simple Gutzwiller treatment.)

Furthermore, the effective mass divergence of EBL has an important physical consequence in the relation between λ^{-2} and T_c [22]. Estimated from $T_c \propto \delta^{2/3}/m^*$ for a free boson gas, one finds $\lambda^{-2} \propto T_c^{1+\beta}$. Therefore, distinct from the simple linear relation expected from standard phase fluctuation scenario, λ^{-2} vs T_c must show a zero slope as T_c approaches zero (since $\beta > 0$). This provides a natural explanation of the super-linear relation in the experimental observations shown in Fig. 4(a) and (c). In fact, with $\beta = 1$ this formula describes very well the observed relation in the entire low- T_c region in both underdoped and overdoped sides.

Such an apparent “symmetry” near the quantum phase transition points between the underdoped and overdoped sides is puzzling within the current lore, given that one is supposedly governed by fluctuation in the phase and the other in the amplitude. Especially, the observed physical properties of the normal-state above T_c in these two regions are quite distinct [28, 33, 34]. In our EBL picture, the contrast in non-superfluid properties is easily understood from the rising importance of the jamming effect discussed above. Concerning the higher-energy features, Fig. 4(d)-(f) show that in the overdoped region the renormalized s -wave (in blue) and d -wave bosons (in red) suffer a significant renormalization, quite distinct from the underdoped and optimally doped region. Yet, the renormalized low-energy coherent d -wave bosonic band near the underdoped (d) and the overdoped transition points becomes heavier (flatter) in a similar fashion (through very different microscopic mechanism though.) In other words, the low-energy phenomenon of superfluidity experiences a similar loss of phase stiffness due to the effective mass divergence despite the distinctly different underlying higher-energy physics.

From this perspective, the non-superconducting “normal state” above 25% doping should have interesting properties. While energetically most favorable locally, the pure d -wave boson would suffer from severe jamming and loss of kinetic energy. It would thus tend to morph into a p -wave boson whose cigar shape allows them to remain mobile at a much larger doping. Therefore, the EBL is expected to behave as an unconventional metal consisting of fluctuating d - and p -wave bosons. Obviously, at very high doping, the electronic correlation will eventually become weaker and the emergent bosons will decompose into weakly bound fermions. However, the observations of well-defined paramagnon at 40% doping [26] and linear resistivity at 30% doping [10] both suggest strongly that such decomposition is not immedi-

ate after the disappearance of superconductivity.

It is also interesting to realize that in every energy scale our EBL experiences important influence of the Mottness of the underlying doped holes through the suppression of their double occupation at each Cu site. First, with the help of kinetic energy, it lays the foundation of near neighboring antiferromagnetic [35] and bi-polaronic [27] correlations that provides a strong tendency to bind doped holes into pairs [24, 36]. Then, it forces the bound pairs to occupy two atomic sites and thus indirectly establishes *d*-wave form [22], since a single-site local pair would necessarily be of *s*-wave. Finally, it produces the extended hard-core constraint of the EBL that ultimately induces jamming of low-energy *d*-wave bosons at high enough density. This jamming in turn suppresses the superfluid phase coherence enough to overcome the increasing density in the overdoped cuprates.

In essence, the recent experiments and our theoretical understanding together produce a clear and complete paradigm for high-temperature superconductivity in cuprates, in great contrast to the current lore. We demonstrate above that the diminishing superfluid stiffness is a natural outcome of jamming in the EBL at around 25–30% doping due to the Mottness of the doped holes. Our study indicates that, in the entire doping range of the superconducting dome, the unconventional superconductivity can be described naturally by the superfluidity of an EBL, without resorting to a crossover into BCS-like amplitude-fluctuating descriptions with weakened pairing interactions. While various observations [10, 37, 38] are already consistent with this new paradigm in the underdoped region, future investigations on the existence of 2e charge quanta of carriers in the overdoped region, for example via shock noise experiments, would provide decisive evidence to this important long-standing puzzle of modern physics.

This work is supported by National Natural Science Foundation of China (NSFC) #11674220 and 11745006 and Ministry of Science and Technology #2016YFA0300500 and 2016YFA0300501. FY acknowledges support from NSFC # 11674025.

* corresponding email: weiku@mailaps.org

- [1] J. G. Bednorz and M., Zeitschrift für Physik B Condensed Matter **64**, 189 (1986).
- [2] J. Bardeen, L. N. Cooper, and J. R. Schrieffer, Phys. Rev. **108**, 1175 (1957).
- [3] V. Z. Kresin and S. A. Wolf, Rev. Mod. Phys. **81**, 481 (2009).
- [4] J. K. Ren, X. B. Zhu, H. F. Yu, Y. Tian, H. F. Yang, C. Z. Gu, N. L. Wang, Y. F. Ren, and S. P. Zhao, Scientific Reports **2**, 248 EP (2012), article.
- [5] N. Miyakawa, P. Guptasarma, J. F. Zasadzinski, D. G. Hinks, and K. E. Gray, Phys. Rev. Lett. **80**, 157 (1998).
- [6] T. Matsuzaki, N. Momono, M. Oda, and M. Ido, Journal of the Physical Society of Japan **73**, 2232 (2004).
- [7] Y. Ando, G. S. Boebinger, A. Passner, L. F. Schneemeyer, T. Kimura, M. Okuya, S. Watauchi, J. Shimoyama, K. Kishio, K. Tamasaku, et al., Phys. Rev. B **60**, 12475 (1999).
- [8] S. Doniach and M. Inui, Phys. Rev. B **41**, 6668 (1990), URL <https://link.aps.org/doi/10.1103/PhysRevB.41.6668>.
- [9] V. J. Emery and S. A. Kivelson, Nature **374**, 434 EP (1995).
- [10] I. Bozovic, X. He, J. Wu, and A. T. Bollinger, Nature **536**, 309 EP (2016).
- [11] J. Zaanen, Nature **536**, 282 EP (2016).
- [12] Y. J. Uemura, L. P. Le, G. M. Luke, B. J. Sternlieb, W. D. Wu, J. H. Brewer, T. M. Riseman, C. L. Seaman, M. B. Maple, M. Ishikawa, et al., Phys. Rev. Lett. **66**, 2665 (1991).
- [13] Y. J. Uemura, Solid State Communications **126**, 23 (2003), cond-mat/0212643.
- [14] Y. J. Uemura, G. M. Luke, B. J. Sternlieb, J. H. Brewer, J. F. Carolan, W. N. Hardy, R. Kadono, J. R. Kempton, R. F. Kiefl, S. R. Kreitzman, et al., Phys. Rev. Lett. **62**, 2317 (1989).
- [15] I. M. Vishik, M. Hashimoto, R.-H. He, W.-S. Lee, F. Schmitt, D. Lu, R. G. Moore, C. Zhang, W. Meevasana, T. Sasagawa, et al., Proceedings of the National Academy of Sciences **109**, 18332 (2012), 10.1073/pnas.1209471109.
- [16] M. Hashimoto, I. M. Vishik, R.-H. He, T. P. Devereaux, and Z.-X. Shen, Nature Physics **10**, 483 EP (2014), review Article.
- [17] T. Kondo, R. Khasanov, T. Takeuchi, J. Schmalian, and A. Kaminski, Nature **457**, 296 EP (2009).
- [18] A. Paramekanti, M. Randeria, and N. Trivedi, Phys. Rev. Lett. **87**, 217002 (2001).
- [19] A. Paramekanti, M. Randeria, and N. Trivedi, Phys. Rev. B **70**, 054504 (2004).
- [20] T. Li and F. Yang, Phys. Rev. B **81**, 214509 (2010).
- [21] Y. Yildirim and W. Ku, Phys. Rev. X **1**, 011011 (2011).
- [22] Y. Yildirim and W. Ku, Phys. Rev. B **92**, 180501 (2015).
- [23] S. Jiang, L. Zou, and W. Ku, arXiv e-prints arXiv:1712.05303 (2017), 1712.05303.
- [24] J. E. Hirsch, Phys. Rev. Lett. **54**, 1317 (1985).
- [25] V. J. Emery, Phys. Rev. B **14**, 2989 (1976).
- [26] M. P. M. Dean, G. Dellea, R. S. Springell, F. Yakhou-Harris, K. Kummer, N. B. Brookes, X. Liu, Y.-J. Sun, J. Strle, T. Schmitt, et al., Nature Materials **12**, 1019 EP (2013).
- [27] A. Alexandrov, *Theory of Superconductivity From Weak to Strong Coupling* (Institute of Physics, 2003).
- [28] E. Dagotto, Rev. Mod. Phys. **66**, 763 (1994).
- [29] M. C. Gutzwiller, Phys. Rev. Lett. **10**, 159 (1963).
- [30] D. S. Rokhsar and B. G. Kotliar, Phys. Rev. B **44**, 10328 (1991), URL <https://link.aps.org/doi/10.1103/PhysRevB.44.10328>.
- [31] See supplementary material.
- [32] D. M. Broun, W. A. Hutmama, P. J. Turner, S. Ozcan, B. Morgan, R. Liang, W. N. Hardy, and D. A. Bonn, Phys. Rev. Lett. **99**, 237003 (2007).
- [33] A. Damascelli, Z. Hussain, and Z.-X. Shen, Rev. Mod. Phys. **75**, 473 (2003).
- [34] D. N. Basov and T. Timusk, Rev. Mod. Phys. **77**, 721 (2005).
- [35] P. W. Anderson, Phys. Rev. **79**, 350 (1950).

- [36] P. W. Anderson, *Science* **316**, 1705 (2007), ISSN 0036-8075.
- [37] F. Mahmood, X. He, I. Božović, and N. P. Armitage, *Phys. Rev. Lett.* **122**, 027003 (2019), URL <https://link.aps.org/doi/10.1103/PhysRevLett.122.027003>.
- [38] A. T. Bollinger, G. Dubuis, J. Yoon, D. Pavuna, J. Misewich, and I. Bozovic, *Nature* **472**, 458 EP (2011).

Supplemental Materials: Mottness induced phase decoherence suggests Bose-Einstein condensation in overdoped cuprate high-temperature superconductors

Zi-Jian Lang, Fan Yang, and Wei Ku

STATISTICAL COUNTING OF GUTZWILLER g -FACTOR

We perform the statistical counting of the Gutzwiller, g -factor $g_{ii'}$, numerically: In a $M = 10 \times 10$ square lattice of the d -wave boson, we randomly places $N \equiv \frac{\delta}{2}M$ bosons and keep only the configurations that satisfied the 13-site extended hard core constraint described in the main text. Within these valid configurations, we then count the probability P of “leagal” hoppings for each first, second and third neighboring hopping $d_i^\dagger d_{i'}$ that do not lead to violation of the constraint afterward.

This probability is closely related to the Gutzwiller g -factor [S1], except that it ignore details of the lowest energy states. Specifically, the definition of the Gutzwiller g -factor involves the ratio of thermal average of the hopping process $g_{ii'} = \langle d_i^\dagger d_{i'} \rangle_c / \langle d_i^\dagger d_{i'} \rangle_0$, evaluated using low-energy states with and without the constraint (denoted by subscripts c and 0 .) In our case, the d_i^\dagger is the creation operator of local d -wave boson. Therefore, this g -factors should conceptually be energy and temperature dependent, especially around the scale of the interaction that induces this constraint. On the other hand, below this energy scale where the constraint is enforced, the g -factor should be quite energy- and temperature-independent, and thus not very sensitive to the detailed structure of the low-lying states. This makes such statistical counting a rather good approximation of the actual g -factor. Indeed, as shown in the main text, the resulting g -factor resembles the VMC calculation very well. This energy independence (within the scale of our low-energy Hamiltonian) also allows us to apply on an approximate ground state in our VMC calculation.

VARIATIONAL MONTE CARLO (VMC) CALCULATION OF GUTZWILLER g -FACTOR

Due to the extremely large many-body Hilbert space of bosonic systems, we can only afford to evaluate the Gutzwiller g -factor using approximate wave function. Luckily, as argued above, the results should be quite insensitive to this choice of approximate wave function. The calculation detail is shown as following:

We calculate the ratio between the expectation values of the hopping term $\langle d_i^\dagger d_{i'} \rangle$ in the “Gutzwiller-projected” Bose-Einstein codensation (BEC) state and that in the mean-field BEC state as the Gutzwiller g -factor, $g_{ii'}$,

$$g_{ii'} = \frac{\langle BEC | P_G d_i^\dagger d_{i'} P_G | BEC \rangle}{\langle BEC | d_i^\dagger d_{i'} | BEC \rangle}. \quad (S1)$$

Here, the P_G represents the extended hard-core constraint imposed on the bosonic hole-pairs, and the BEC mean-field state $|BEC\rangle$ is expressed by the following normalized formula,

$$|BEC\rangle \equiv \frac{1}{\sqrt{N!}} (d_{\mathbf{k}=0}^\dagger)^N |0\rangle = \frac{1}{\sqrt{N!}} \left(\frac{1}{\sqrt{M}} \sum_{i=1}^M d_i^\dagger \right)^N |0\rangle, \quad (S2)$$

where M and N represent the total site number and boson numbers respectively, with $N = M\delta/2$.

The denominator of Eq.(S1) can be easily obtained as,

$$\langle BEC | d_i^\dagger d_{i'} | BEC \rangle = \frac{1}{M} \sum_{\mathbf{k}} e^{-i\mathbf{k} \cdot (\mathbf{R}_i - \mathbf{R}_{i'})} \langle BEC | d_{\mathbf{k}}^\dagger d_{\mathbf{k}} | BEC \rangle = \frac{1}{M} \langle BEC | d_0^\dagger d_0 | BEC \rangle = \frac{N}{M} = \delta/2. \quad (S3)$$

The numerator of Eq.(S1) can be evaluated as,

$$\langle BEC | P_G d_i^\dagger d_{i'} P_G | BEC \rangle = \sum_{\alpha} |\langle \alpha | P_G | BEC \rangle|^2 \sum_{\beta} \langle \alpha | d_i^\dagger d_{i'} | \beta \rangle \cdot \frac{\langle \beta | P_G | BEC \rangle}{\langle \alpha | P_G | BEC \rangle} \equiv \sum_{\alpha} P_{\alpha} B_{\alpha}, \quad (S4)$$

where $P_{\alpha} \equiv |\langle \alpha | P_G | BEC \rangle|^2$ represents the weight of each configuration $|\alpha\rangle$ in the Gutzwiller-projected wave function $P_G |BEC\rangle$, and $B_{\alpha} = \sum_{\beta} \langle \alpha | d_i^\dagger d_{i'} | \beta \rangle \cdot \frac{\langle \beta | P_G | BEC \rangle}{\langle \alpha | P_G | BEC \rangle}$ represents the measurement for the configuration $|\alpha\rangle$. The weight

P_α and the measurement B_α for any configuration $|\alpha\rangle$ are easily obtained. From Eq.(S2), one easily finds that the weights P_α for all the configurations $|\alpha\rangle$ which are permitted by the extended hard-core constraint are equal, while those for the constraint-prohibited configurations are zero. The value B_α of any constraint-permitted configuration $|\alpha\rangle$ is as such: defining $|\beta\rangle = d_i^\dagger d_i |\alpha\rangle$, if configuration $|\beta\rangle$ is permitted by the extended hard-core constraint then $B_\alpha = 1$; otherwise $B_\alpha = 0$. These formulae provide appropriate start-point for the following Monte-Carlo calculations.

In the Monte-Carlo calculation, we start from an arbitrarily given configuration $|\alpha_1\rangle$. Then randomly selecting a particle in that configuration, we let the particle hop to any other hard-core-constraint-permitted position on the lattice to obtain a second configuration $|\alpha_2\rangle$. This completes an update. Continuing the updates, we obtain a configuration series $|\alpha_1\rangle, |\alpha_2\rangle, |\alpha_3\rangle, \dots$. After about 10^4 Monte-Carlo steps, the thermalization can be realized. In the succeeding Monte-Carlo steps, one begins to extract the measurement B_α for the configuration $|\alpha\rangle$, and to average these B_α to obtain the numerator defined by Eq.(S4). To avoid auto-correlation, we take one measurement after each N Monte-Carlo steps. About 10^5 measurements are performed to attain convergence. The final result for the Gutzwiller g -factor is given by Eq.(S1), Eq.(S3) and Eq.(S4).

* corresponding email: weiku@mailaps.org
 [S1] M. C. Gutzwiller, Phys. Rev. Lett. **10**, 159 (1963).